

**ALL-SILICON CARBIDE HYBRID WIRELESS-WIRED OPTICS
TEMPERATURE SENSOR NETWORK BASIC DESIGN ENGINEERING
FOR POWER PLANT GAS TURBINES**

Nabeel A. Riza and Mumtaz Sheikh

QUERY SHEET

This page lists questions we have about your paper. The numbers displayed at left can be found in the text of the paper for reference. In addition, please review your paper as a whole for corrections.

AQ1: Au: Please provide page range.

TABLE OF CONTENTS LISTING

The table of contents for the journal will list your paper exactly as it appears below:

All-Silicon Carbide Hybrid Wireless-Wired Optics Temperature
Sensor Network Basic Design Engineering for Power Plant Gas
Turbines **Nabeel A. Riza and Mumtaz Sheikh**

ALL-SILICON CARBIDE HYBRID WIRELESS-WIRED OPTICS TEMPERATURE SENSOR NETWORK BASIC DESIGN ENGINEERING FOR POWER PLANT GAS TURBINES

Nabeel A. Riza and Mumtaz Sheikh

*Photonic Information Processing Systems Laboratory,
College of Optics & Photonics-CREOL, University of Central Florida,
Orlando, Florida, USA*

Proposed is a novel design of a fiber-remoted temperature sensor network for operation in the extreme environments of power generation gas turbines. The network utilizes a robust all-Silicon Carbide wireless-wired hybrid temperature probe design that features an all-passive front-end, active laser beam targeting, and the use of an optical wedge that eliminates optical interferometric noise in addition to serving as a partial vacuum window for the probe cavity to minimize laser beam wander due to air turbulence. An example basic network is built at the 1550nm band using 1 × 2 micro-electro-mechanical systems (MEMS) fiber-optic switches with engineered sensor system robust performance observed at 1000°C using a custom assembled all-SiC probe with a Magnesium Fluoride (MgF₂) high temperature window.

Keywords: extreme environments, gas turbines, optical sensor, silicon carbide, temperature sensor

1. INTRODUCTION

Next generation greener power plant gas turbines are being designed to operate at extremely high temperatures (Ausubel 2004). Presently, power plants use thermocouple technology for temperature monitoring in gas turbines to keep them operating under optimal conditions. However, the platinum-rhodium tip thermocouples deployed are susceptible to reliability and limited lifetime issues. Other alternatives, including optics have therefore been proposed to overcome these thermocouple limitations. Optical thermometers include advanced silica (Grobnic et al. 2004a), sapphire (Grobnic et al. 2004b; Zhang et al. 2004), and SiC-based (Beheim 1986; Cheng et al. 2003) temperature sensors. Advanced silica-based sensors can measure temperatures up to ~1000°C, limited by Fiber Bragg Grating (FBG) erasure beyond ~1000°C. Sapphire-based sensors have issues such as multimodal optical interference, polarization sensitivity, as well as non-thermally matched components in the sensor frontend that limit overall long-term performance. Early SiC sensors using SiC thin films (Beheim 1986; Cheng et al. 2003) on silicon or sapphire substrates also suffer from the same problem

Address correspondence to Nabeel A. Riza, Photonic Information Processing Systems Laboratory, College of Optics & Photonics-CREOL, University of Central Florida, 4000 Central Florida Blvd., Orlando, FL 32816-2700, USA. E-mail: riza@creol.ucf.edu

NOMENCLATURE

N Number of all-SiC probes n Refractive index R_{FP} Optical reflectance of SiC chip R_1 Front surface reflectance of SiC chip R_2 Back surface reflectance of SiC chip T Temperature of the SiC chip t Thickness of the SiC chip	λ Wavelength of incident light ϕ Optical path length difference θ_w Angle of the MgF ₂ wedge θ_a Transmission angle at front surface of MgF ₂ θ_b Incidence angle at back surface of MgF ₂ θ_i Incident angle of laser beam on MgF ₂ θ_t Transmission angle of beam after passing through MgF ₂
---	--

of Coefficient of Thermal Expansion (CTE) un-matched sensor frontend design that can lead to mechanical breakdown over sensor life-time. Recently, a micro-machined grating inside bulk SiC has also been used to demonstrate temperature sensing up to 399°C (DesAutels et al. 2008), though the technique still needs to be developed for use in a >1000°C gas turbine extreme environment. To address prior-art sensor limitations, recently proposed is a hybrid wireless-wired approach using an all-SiC frontend probe to enable extreme temperature sensing for gas turbines (Riza et al. 2006, 2007; Riza and Sheikh 2008; Sheikh and Riza 2008, 2009). The all-SiC probe uses a single crystal SiC chip embedded inside a sintered SiC tube to overcome the problem of unmatched CTEs in the sensor frontend. References (Riza et al. 2006, 2007; Riza and Sheikh 2008; Sheikh and Riza 2008, 2009) give detailed temperature sensing and probe performance results for the individual all-SiC probe using an oven in the laboratory. The individual all-SiC probe has also been subjected to extreme environment tests in a Siemens combustion test rig with temperature measurements up-to the 1200°C level and probe operations in 20 atm turbine pressure range with sulphuric acid rich chemically caustic conditions (Riza and Sheikh 2009; Riza et al. 2010).

From a practical applications point-of-view, it is very attractive to have a sensor system that has many distributed or independent physical location sensors such as the mentioned extreme gas turbine environment temperature sensors within a large electric power plant. Having a discrete sensor location distributed network can not only build redundancy-based fault-tolerance in the network, but it also provide an intelligent platform to accurately access the real-time health status of the given platform (e.g., gas turbine) to prevent catastrophic failure and costly complete shut down. Previous works on discrete distributed sensors have mainly focused on using parallel and serial all-fiber interconnections between the individual sensors (Koo and Kersey 1995; Li et al. 2003). The individual discrete location sensors are generally accessed using Wavelength Division Multiplexing techniques involving specific wavelength lasers or wavelength-selective active optics. The key point to note is that operation of such fiber sensing networks requires special extreme (chemical, pressure, and temperature) environment packaging of not only the optical fibers but also the discrete fiber sensing devices (e.g., Fiber Bragg Gratings), making such all-fiber distributed discrete locations sensor systems highly susceptible to failure due to fiber degradation effects.

The purpose of this article is to show how the recently proposed all-SiC probes can be utilized to engineer a basic fiber-remoted temperature sensing network for

95 gas turbine applications. Specifically, the probe is designed with novel features that
 96 allows the optical fibers to terminate well before the hot zones of the gas turbine,
 97 importantly letting the wireless light make the final temperature sensing connection
 98 with the super hot SiC optical chip embedded deep inside the inserted all-SiC
 99 probe. The article describes the special design of the probe and its fundamental
 100 interconnecting networked system allowing the formation of a high optical efficiency
 101 and cost-effective system. An example basic sensor system is built in the laboratory
 102 and key system features are tested to highlight system operational robustness. Note
 103 that while the details of the temperature sensing principle and the performance
 104 results of the individual all-SiC probe are reported in references (Riza et al. 2006,
 105 2007, 2010; Riza and Sheikh 2008, 2009; Sheikh and Riza 2008, 2009), this article
 106 focuses on how the previously tested SiC optical probe can be engineered via several
 107 presented critical design innovations that allow the sensor's use in an industrial
 108 temperature sensing scenario.

110 2. FIBER REMOTED TEMPERATURE SENSING NETWORK 111 USING ALL-SiC PROBES

112 Figure 1 shows the proposed novel temperature sensing network design for
 113 gas turbines in electric power plants indicating the use of N all-SiC temperature
 114 sensing probes that are inserted in the turbine extreme environment. To put things
 115 in perspective, the typical combustor section of a gas turbine can have $N < 20$ gas
 116 temperature sensing points located symmetrically around the gas flow path. For
 117 these advanced next generation clean coal-fired combined cycle power plants, the
 118 combustor gas firing temperatures reach 1500°C such as for Siemens SGT6-6000G
 119 turbine. Today, this extreme temperature sensing for test engines is typically done
 120 using custom packaged high temperature (870°C to 1700°C rating) type B Platinum-
 121 Rhodium metal thermocouple probes with each probe typically 61 cm (24 inches) in
 122 length. Thus, each thermocouple has sufficient length to pass through the combustor
 123 refractory (thermal insulation) concentric layers that isolate the innermost extremely
 124 hot gas section from the external ambient conditions (e.g., $<70^{\circ}\text{C}$) instrumentation
 125

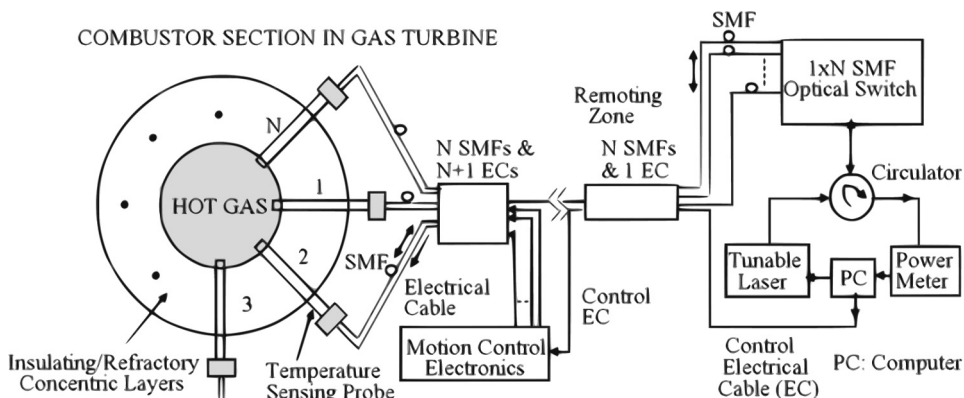


Figure 1. Proposed N temperature probes sensor network using the All-Silicon Carbide Hybrid Wireless-Wired Optics Temperature Sensors.

142 zone where plant technicians operate. The proposed Figure1 design takes advantage
 143 of this operational scenario by first using an insertable all-SiC probe to reach the
 144 hot section, much like a thermocouple tip and two, using fiber-optics only in the
 145 friendlier external instrumentation zone. Hence, each all-SiC probe has one Single
 146 Mode Fiber (SMF) to remote laser light and one Electrical Cable (EC) for the fiber
 147 motion mechanics control. For N probes, the N electrical cables are connected to
 148 the motion control electronics positioned near the turbine instrumentation bay. On
 149 the other hand, the N single mode fibers connected to the probes are gathered and
 150 routed as one N-fiber optical cable that leads to a remote control site in the plant.
 151 The optical cable also shares its mechanical cable encasing with an electrical cable
 152 that connects the remote control computer with the motion control electronics. The
 153 N single mode fibers connect to a $N \times 1$ Fiber-Optic (FO) switch that connects
 154 to a 3-port fiber-optic circulator. A computer controlled tunable laser connected
 155 to the circulator forms the laser light source for the distributed sensor network
 156 with the optical detector connected to the other port of the circulator forming the
 157 optical detection arm. The tunable laser is needed in order to interrogate the SiC
 158 chip at multiple laser wavelengths, a requirement for the previously demonstrated
 159 temperature sensing technique (Riza et al. 2006; Riza and Sheikh 2008; Sheikh and
 160 Riza 2009). Control of the fiber-optic switch decides which one of the N all-SiC
 161 probes is lit to sense the turbine zone temperature. Because both tunable lasers,
 162 detectors, and mechanics-based fiber-optic switches can be reset at moderately fast
 163 times, e.g., milliseconds, fast multi-sensor signal processing can be economically
 164 implemented for the complete gas turbine using the same transmit-receive optical
 165 hardware.

166 The deployed all-SiC probe temperature sensing technique relies on measuring
 167 the change in the temperature dependent refractive index and thickness of the
 168 embedded SiC chip by optically interrogating it at normal incidence using a tunable
 169 infrared laser. The SiC chip acts a natural Fabry-Perot (FP) interferometer whose
 170 optical reflectance is given by:

$$171 R_{FP} = \frac{R_1 + R_2 + 2\sqrt{R_1 R_2} \cos \varphi}{1 + R_1 R_2 + 2\sqrt{R_1 R_2} \cos \varphi}. \quad (1)$$

172 Here $\varphi = \frac{4\pi}{\lambda} n(\lambda, T)t(T)$, where $n(\lambda, T)$ is the chip refractive index at wavelength
 173 λ and chip temperature T , $t(T)$ is the chip thickness at temperature T , and R_1 and R_2
 174 are the classic Fresnel reflection coefficients for the SiC-air interface. As described
 175 previously (Riza et al. 2006; Riza and Sheikh 2008; Sheikh and Riza 2009), by
 176 measuring the SiC chip reflectance at multiple wavelengths, the temperature of the
 177 chip is unambiguously determined.
 178

179 To enable the proposed Figure 1 network design, one must deploy a novel
 180 hybrid wireless-wired probe design as shown in Figure 2(a). The probe consists of
 181 one long sintered-SiC material hollow tube with a single crystal SiC optical chip
 182 packaged on the tube hot end and the cooler open end connected to a steel flat-
 183 flange style high pressure connector using a high temperature sealing ring. The steel
 184 connector has threads that screw into a pressurized turbine inlet port where the
 185 all-SiC probe is inserted for temperature measurements. The flat steel flange seats
 186 an optical window through which the laser beam enters to strike the SiC optical
 187 chip. A key probe design feature is the use of a high temperature optical wedge
 188

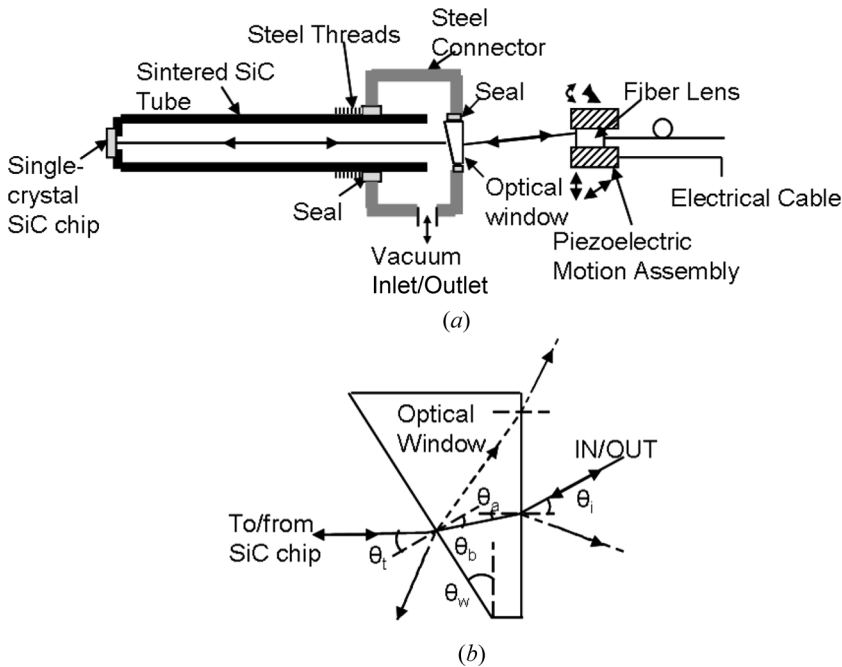


Figure 2. (a) Proposed all-passive frontend temperature probe design with its active motion control back-end. (b) Crosstalk eliminated wireless optical beam path design using an optical window designed as a high temperature optical wedge.

as the window. As shown in Figure 2(b), the wedge acts to separate the unwanted light beams coming from the various window reflections from the temperature coded retro-reflected light beam coming from the SiC chip. This is a critical probe design feature as it eliminates the temperature dependent optical crosstalk from the window optics multiple Fresnel reflections. Another probe design feature is the use of a vacuum inlet/outlet port to maintain a partial vacuum with the probe internal cavity. This is a critical design innovation as it essentially eliminates air-based laser beam turbulence and beam motion within the front-end tube, thus allowing stable targeting of the SiC chip. To enable this reliable targeting, the back-end of the probe also features a smart light targeting system where the fiber lens is mounted in precision motion mechanics with tip/tilt and translational controls. Because one is dealing with a single mode fiber and a wireless laser beam for both transfer and reception of light, although at a short travel distance, coupling is highly sensitive to beam alignment including sub-degree tilts (van Buren and Riza 2003). Beam alignment can easily get spoilt in an extreme environment due to mechanical shocks and vibrations. In this industrial environment, computer controlled fiber lens motion mechanics is needed to restore ideal beam alignment. Thus, the fiber lens motion mechanics maintains chip targeting to take reliable optical readings. A partial vacuum also reduces convection-based heat transfer from the SiC chip that can lead to unwanted chip cooling. The back end of the probe with the fiber-optics is thermally isolated from the probe front-end, enabling reliable use of standard fiber-optics with typical ratings of $<70^{\circ}\text{C}$. For example, the probe-back end can be

connected to the turbine external interfaces near the pressurized inlet where various instruments are mounted.

3. EXPERIMENTAL RESULTS

The purpose of the experiment is to demonstrate a proof-of-concept Figure 1 sensor network design to test the proposed system and probe innovations. Figure 3 shows the assembled all-SiC probe provided by our partner Nuonics, Inc. The probe has a ~ 400 micron embedded SiC optical chip at its end with a probe length, inner diameter, and outer diameter of 41.5cm, 2.1cm, and 3.3cm, respectively. A Viton (205°C max temperature) seal is used in the steel connector with a 2.54cm diameter MgF₂ wedge (index $n = 1.37$) with a $\theta_w = 3^\circ$ wedge angle. Using Figure 2b, geometry, and applying Snell's law, one can write: $\sin \theta_i = n \sin \theta_a$, $\theta_b = \theta_w - \theta_a$, $\sin \theta_t = n \sin \theta_b$, and $\theta_t = \theta_w$. Given $\theta_w = 3^\circ$, $n = 1.37$, $\theta_t = 3^\circ$, one can compute $\theta_b = 2.2^\circ$, $\theta_a = 0.8^\circ$, and the incident angle $\theta_i = 1.1^\circ$ required for proper beam launch from the Fiber Lens (FL). The fiber lens has a 60cm designed half-self-imaging distance (van Buren and Riza 2003) producing a 550micron $1/e^2$ spot size on the SiC chip. The fiber lens has an 8mm outer diameter housing and the fiber lens is connected to 9/125 micron standard 1550nm single mode fiber. The single mode fiber is packaged in a 3mm diameter stainless steel cable 15m in length. The single mode fiber is connected to an output port of a miniature 1×2 Hitachi MEMS MS204-P switch that is interconnected to another 1×2 MEMS switch that in-turn forms a $1 \times N$ switch; in this case, $N = 3$ output ports. For $N = 16$ ports, 4 cascading layers of 1×2 switches can be used with one way in-to-out port loss expected to be a reasonable $0.7 \text{ dB/switch} \times 4 \text{ stages} = 2.8 \text{ dB}$. The switch resets in $<5 \text{ ms}$ using a 5V pulse and has a -60 dB crosstalk level. The input switch port is connected to a circulator that connects one port to a Santec tunable laser and another port to a Newport optical power meter. The fiber lens is mounted in a computer controlled tip/tilt and 2-axis translation stages Standa Models 8MBM24-2 and 8MT173-20 with a <1 arcsec tilt resolution and $1.25 \mu\text{m}$ translation resolution.

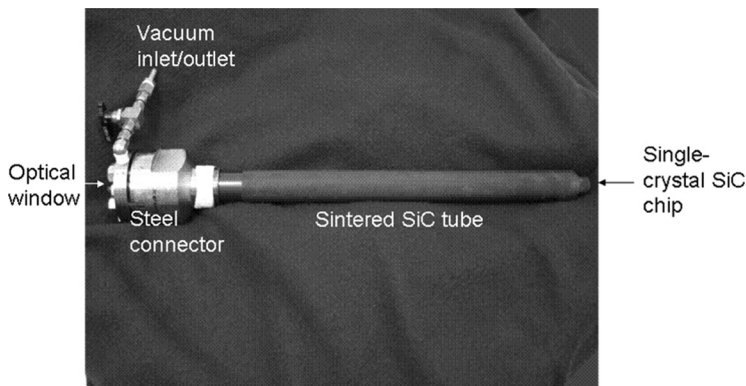


Figure 3. All-SiC temperature sensing probe assembly deployed in system test.

283
 284
 285
 286
 287
 288
 289
 290
 291
 292
 293
 294
 295
 296
 297
 298
 299
 300
 301
 302
 303
 304
 305
 306
 307
 308
 309
 310
 311
 312
 313
 314
 315
 316
 317
 318
 319
 320
 321
 322
 323
 324
 325
 326
 327
 328
 329

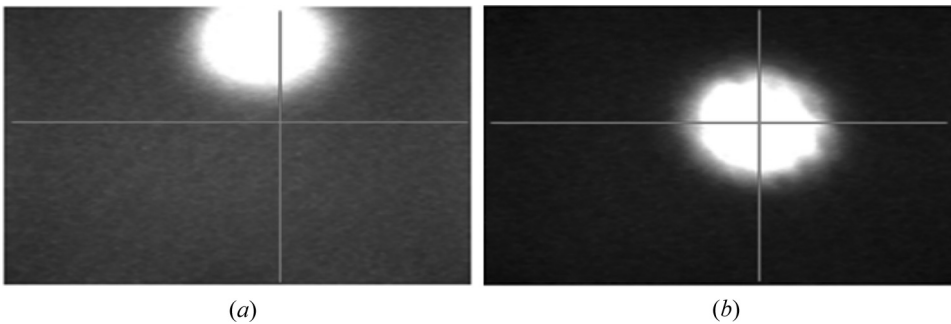


Figure 4. At 1000°C, SiC chip reflected 1550nm laser beam motion when (a) the probe cavity is open to external conditions, and (b) when the probe cavity maintains a partial vacuum. Image is 8.8 mm × 6.6 mm.

The probe is inserted into an oven that is heated to 1000°C. Using a camera and a beam splitter in the free-space path between window and fiber lens, the received temperature coded beam is observed. In Figure 4, the stable target zone is indicated by the intersection of the horizontal and vertical lines. Figure 4(a) shows that the infrared beam has spatially moved off the stable target zone, hence greatly disrupting the ideal light coupling conditions for the fiber lens-single mode fiber assembly. To test the proposed probe innovation, a hand operated vacuum pump is connected to the probe cavity and a 25 inch-Hg (85 kpa) partial vacuum is obtained. As shown in Figure 4(b), the beam position is on target and becomes stable at the fiber lens for optimal coupling. Hence, Figure 4(b) shows how maintaining a partial vacuum inside the probe cavity ensures that the retro-reflected beam off the SiC

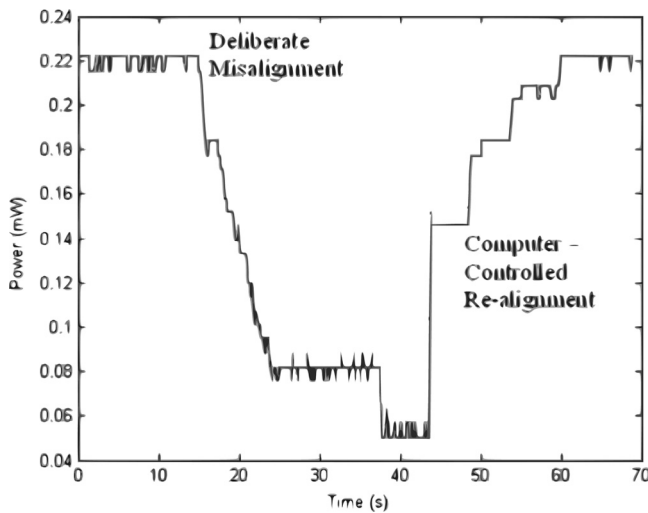


Figure 5. Time trace of reflected power off the SiC chip in the probe when the system is deliberately misaligned and then re-aligned using computer-controlled fiber lens motion stages.

330 chip stays within a target zone on the fiber lens instead of moving off that target
331 zone as is the case in Figure 4(a) with no vacuum inside the cavity.

332 Figure 5 shows a time trace of the SiC chip reflected optical power coupled
333 back into the fiber lens. Initially, the probe is perfectly aligned with the fiber lens
334 and all the light reflected off the SiC chip is coupled back into the fiber. Next,
335 the probe is slightly misaligned to simulate the effect of mechanical shocks or
336 vibrations, a common occurrence in industrial environments, causing a large loss in
337 the single mode fiber coupled optical power (see Figure 5). Since the temperature
338 sensing methodology (Riza et al. 2006; Riza and Sheikh 2008; Sheikh and Riza 2009,
339 2008; Riza et al. 2007) relies on receiving a sufficient power level signal off the SiC
340 chip, a large loss in the single mode fiber coupled optical power would result in
341 significant errors in temperature measurement given reduced modulation depth of
342 the interferometric signal. Finally, the active computer controlled alignment process
343 is activated and full single mode fiber power coupling is recovered (see Figure 5)
344 indicating the robustness of the probe design. The fiber-optic switches are also
345 controlled to light all three test probe channels. The total system optical loss from
346 laser to detector is measured to be 11 dB, indicating a low power 10 mW laser
347 is adequate for sensor operation. Note that the temperature sensing and probe
348 performance results for the individual all-SiC probe have already been presented
349 (Riza and Sheikh 2008, 2009; Sheikh and Riza 2008, 2009; Riza et al. 2007, 2010).

351 4. CONCLUSION

352 For the first time, to the authors' knowledge, shown is the design engineering
353 of a temperature sensor network for gas turbines using the proposed all-SiC probe
354 technology using both wired (fiber) and wireless (freespace) optics. The probe has
355 been designed, assembled, and tested within the context of a fiber remoted discrete
356 location sensor network, highlighting its novel operation features for robustness via
357 active beam alignment and partial vacuum controls.

359 REFERENCES

- 360 Ausubel, J. H. 2004. Big green energy machines. *The Industrial Physicist* 10(5):20–24.
361 Beheim, G. 1986. Fibre-optic thermometer using semiconductor-etalon sensor. *Electron. Lett.*
362 22(5):238–239.
363 Cheng, L., A. J. Steckl, and J. Scofield. 2003. SiC thin film Fabry-Perot interferometer for
364 fiber-optic temperature sensor. *IEEE Tran. Electron Devices* 50(10):2159–2164.
365 DesAutels, G. L., P. Powers, C. Brewer, M. Walker, M. Burky, and G. Anderson. 2008.
366 Optical temperature sensor and thermal expansion measurement using a femtosecond
367 micromachined grating in 6H-SiC. *Appl. Opt.* 47(21):3773–3777.
368 Grobncic, D., C. W. Smelser, S. J. Mihailov, and R. B. Walker. 2004a. Isothermal behavior
369 of fiber Bragg gratings made with ultrafast radiation at temperatures above 1000°C.
370 *European Conf. Opt. Comm. (ECOC) Proc.* 2:130–131.
371 Grobncic, D., S. J. Mihailov, C. W. Smelser, and H. Ding. 2004b. Ultra high temperature
372 FBG sensor made in sapphire fiber using isothermal femtosecond laser radiation.
373 *European Conf. Opt. Comm. (ECOC) Proc.* 2:128–129.
374 Koo, K. P. and A. D. Kersey. 1995. Bragg grating based laser sensors systems with
375 interferometric interrogation and wavelength division multiplexing. *J. Lightwave Tech.*
376 13(7):1243–1249.

- 377 Li, W., D. C. Abeysinghe, and J. T. Boyd. 2003. Wavelength multiplexing of
378 microelectromechanical system pressure and temperature sensors using fiber Bragg
379 gratings and arrayed waveguide gratings. *Optical Eng.* 42(2):431–438.
- 380 Riza, N. A. and M. Sheikh. 2008. Silicon carbide based extreme environment temperature
381 sensor using wavelength tuned signal processing. *Optics Letters* 33(10):1129–1131.
- 382 Riza, N. A. and M. Sheikh. 2009. All-silicon carbide hybrid wireless-wired optics
383 temperature sensor: Turbine tests and distributed fiber sensor network design. *SPIE*
384 *Photonics Europe Conf. on Optical Sensors Proc.* 7356:73560O–73560O-5.
- 385 Riza, N. A., M. A. Arain, and F. A. Perez. 2006. Harsh environments minimally invasive
386 optical sensor using freespace targeted single crystal silicon carbide. *IEEE Sensors*
387 *Journal* 6(3):672–685.
- 388 Riza, N. A., M. Sheikh, and F. Perez. 2007. Design and fabrication of an extreme
389 temperature sensing optical probe using silicon carbide technologies. *IEEE Sensors*
390 *Conference Proc.* I-4244-1262-5/07:660–663.
- 391 Riza, N. A., M. Sheikh, and F. Perez. 2010. Hybrid wireless-wired optical sensor for extreme
392 temperature measurement in next generation energy efficient gas turbines. *ASME J. Eng.*
393 *Gas Turbines Power* 132 (in press).
- 394 Sheikh, M. and N. A. Riza. 2009. Direct measurement high resolution wide range extreme
395 temperature optical sensor using an all-silicon carbide probe. *Opt. Lett.* 34(9):1402–1404.
- 396 Sheikh, M. and N. A. Riza. 2008. Experimental studies of an all-silicon carbide hybrid
397 wireless-wired optics temperature sensor for extreme environments in turbines. *SPIE*
398 *Optical Sensing IV Conf. Proc.* 7003:70030C-70030C–10.
- 399 van Buren, M. and N. A. Riza. 2003. Foundations for low loss fiber gradient-index lens pair
400 coupling with the self-imaging mechanism. *Applied Optics* 42(3):550–565.
- 401 Zhang, Y., G. R. Pickrell, B. Qi, A. S.-Jazi, and A. Wang. 2004. Single-crystal sapphire-based
402 optical high temperature sensor for harsh environments. *Opt. Eng.* 43(1):157–164.
- 403
- 404
- 405
- 406
- 407
- 408
- 409
- 410
- 411
- 412
- 413
- 414
- 415
- 416
- 417
- 418
- 419
- 420
- 421
- 422
- 423

AQ1